Journal of Zhejiang University SCIENCE A
ISSN 1673-565X (Print); ISSN 1862-1775 (Online)
www.zju.edu.cn/jzus; www.springerlink.com
E-mail: jzus@zju.edu.cn

Investigation on short-term burst pressure of plastic pipes reinforced by cross helically wound steel wires*

Jin-yang ZHENG†, Yong-jian GAO, Xiang LI, Xiu-feng LIN, Yu-bin LU, Yan-cong ZHU

(*Institute of Chemical Machinery and Process Equipment, Zhejiang University, Hangzhou 310027, China*)

†E-mail: jyzh@zju.edu.cn

Received Sept. 6, 2007; revision accepted Jan. 21, 2008; published online Apr. 15, 2008

Abstract: Plastic pipes reinforced by cross helically wound steel wires (PSP), which have exhibited excellent mechanical performance, consist of inner polyethylene (PE) layer, winding layer and outer PE layer. The winding layer is composed of two monolayers where steel wires are cross helically wound. An analytical procedure is developed to predict the short-term burst pressure of PSP as the monolayer is assumed to be elastic and orthotropic. The 3D anisotropic elasticity and Maximum Stress Failure Criterion are employed in the formulation of the elasticity problem. Good agreement between the theoretical results and the experimental data shows that the proposed approach can well predict the short-term burst pressure of PSP.

Key words: Composite pipes, Maximum Stress Criterion, Short-term burst pressure
doi:10.1631/jzus.A071476 **Document code:** A **CLC number:** TQ320

INTRODUCTION

Plastic pipes reinforced by cross helically wound steel wires (PSP), a new type of plastic-matrix steel composite pipes developed in China, is being extensively used in areas of petroleum, chemical engineering and municipal water supply, etc. (Lu *et al.*, 2005; Zheng *et al.*, 2007). As shown in Fig.1, steel wire mesh skeleton is sandwiched in the middle joined thermoplastic polyethylene (PE) on the inside and outside of the pipe wall. The skeleton is formed by cross wound high strength steel wires which are integrated with PE by high performance cohesive resin. By combining the advantages of both plastic and metal, the PSP has many potential properties such as high stiffness and strength, good corrosion resistance and thermal insulation. The PSP consists of three continuous layers, i.e., inner PE layer, winding layer and outer PE layer. The composite layer is considered to be a laminated structure, constituted by upper and lower monolayers (Zheng *et al.*, 2006), as shown in Fig.2.

Prediction of the burst pressure of PSP for a critical application is an important consideration in its design for safety and reliability. To obtain a more realistic indication of the margin of safety available over the maximum expected operating pressure (MEOP), it is very necessary to explore the value of burst pressure. Considering the time dependent behaviour of the PE, there exist short-term and long-term failure modes, in which the PE is modelled as a linear elastic material and a viscoelastic material, respectively (Kruijer *et al.*, 2006). This research is mainly concerned with the short-term failure behaviour of PSP.

There have been many researches on mechanical response of composite structures under internal pressure. The composite structures have a similar structure to PSP. Xia *et al.*(2001a; 2001b) developed the stress analysis of the filament wound sandwich pipes under internal pressure based on the 3D classical lamination theory. Parnas and Katirci (2002) also conducted the stress analysis of the fiber-reinforced

* Project supported by the New Century Excellent Talents in University, MOE, China (No. NCET-04-0526), the Specialized Research Fund for the Doctoral Program of Higher Education, MOE, China (No. J20050398), and the Key Project of Wenzhou (No. G2004034), China

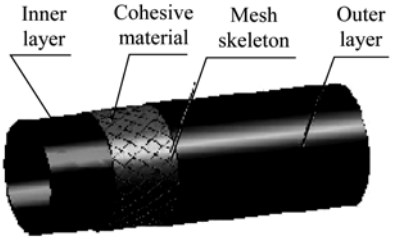

Fig.1 Structure of PSP

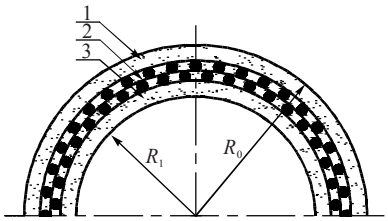

1: Outer layer; 2: Winding layer; 3: Inner layer

Fig.2 Schematic diagram of PSP's cross-section

composite pressure vessels subjected to internal pressure. Kobayashi *et al.*(2007) proposed an elastic-plastic analysis on the filament wound carbon fiber-reinforced composite pipes by applying partially plastic thick-walled cylinder theory. The probabilistic analysis combined with progressive failure analysis is developed by Uemura and Hwang to predict the short-term burst pressure of a composite pressure vessel (Uemura and Fukunaga, 1981; Hwang *et al*., 2003).

Provided that the interfaces between the steel wire and PE are perfectly bonded, the strain of the steel wire and PE in the steel wound direction can be considered to be equal. Because the Young's modulus of the steel wire is far greater than that of PE, the stresses in the steel wires are much greater than those in the PE. When the PSP is subjected to internal pressure, steel wires first reach their strength limits and break, resulting in that the PSP loses the reinforcement of the steel wire mesh skeleton and bursts in a short-term. It can be concluded that the winding layer containing the steel wire mesh skeleton determines the PSP's burst resistance.

In this research, the authors propose that short-term burst pressure of PSP is just the internal pressure when steel wires reach their strength limits. By applying the 3D anisotropic elasticity and Maximum Stress Failure Criterion, a new solution for predicting short-term burst pressure of PSP is presented.

THRORETICAL CALCULATION FOR SHORT-TERM BURST PRESSURE

Multi-layer elastic analysis

The monolayer, basic mechanical analysis unit of winding layer, has three symmetrical performance planes and is orthotropic. As shown in Fig.3, the material coordinate system of the monolayer is designated as (L, T, r), where L is the steel wound direction, T is the direction vertical to the steel wire in plane, and r is the normal direction of the monolayer. The cylindrical coordinate system is designated as (z, θ, r), where z, θ, r is the axial, circumferential and radial direction of PSP, respectively. The two coordinate systems have the same coordinate direction of r, and α is the angle between L and z direction.

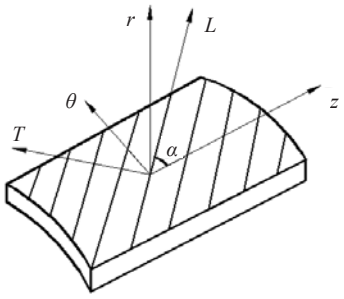

Fig.3 Relation of material coordinate and cylindrical coordinate system

The stress-strain relations of the kth layer in the cylindrical coordinate system is given as

$$\boldsymbol{\varepsilon}_z^{(k)} = \overline{\boldsymbol{S}}^{(k)} \boldsymbol{\sigma}_z^{(k)}, \tag{1}$$

where

$$\boldsymbol{\varepsilon}_z^{(k)} = \left\{ (\varepsilon_z \quad \varepsilon_\theta \quad \varepsilon_r \quad \gamma_{\theta r} \quad \gamma_{rz} \quad \gamma_{z\theta})^{(k)} \right\}^{\mathrm{T}}, \tag{2}$$

$$\boldsymbol{\sigma}_z^{(k)} = \left\{ (\sigma_z \quad \sigma_\theta \quad \sigma_r \quad \tau_{\theta r} \quad \tau_{rz} \quad \tau_{z\theta})^{(k)} \right\}^{\mathrm{T}}, \tag{3}$$

$$\overline{\boldsymbol{S}}^{(k)} = \begin{bmatrix} \overline{S}_{11} & \overline{S}_{12} & \overline{S}_{13} & 0 & 0 & 0 \\ \overline{S}_{12} & \overline{S}_{22} & \overline{S}_{23} & 0 & 0 & 0 \\ \overline{S}_{13} & \overline{S}_{23} & \overline{S}_{33} & 0 & 0 & 0 \\ 0 & 0 & 0 & \overline{S}_{44} & 0 & 0 \\ 0 & 0 & 0 & 0 & \overline{S}_{55} & 0 \\ 0 & 0 & 0 & 0 & 0 & \overline{S}_{66} \end{bmatrix}^{(k)}. \tag{4}$$

The stress-strain relations of the kth layer in the material coordinate system is given as

$$\boldsymbol{\varepsilon}_L^{(k)} = \boldsymbol{S}^{(k)} \boldsymbol{\sigma}_L^{(k)}, \tag{5}$$

where

$$\boldsymbol{\varepsilon}_L^{(k)} = \left\{ (\varepsilon_L \quad \varepsilon_T \quad \varepsilon_r \quad \gamma_{Tr} \quad \gamma_{rL} \quad \gamma_{LT})^{(k)} \right\}^{\mathrm{T}}, \tag{6}$$

$$\boldsymbol{\sigma}_L^{(k)} = \left\{ (\sigma_L \quad \sigma_T \quad \sigma_r \quad \tau_{Tr} \quad \tau_{rL} \quad \tau_{LT})^{(k)} \right\}^{\mathrm{T}}, \tag{7}$$

$$\boldsymbol{S}^{(k)} = \begin{bmatrix} S_{11} & S_{12} & S_{13} & 0 & 0 & 0 \\ S_{12} & S_{22} & S_{23} & 0 & 0 & 0 \\ S_{13} & S_{23} & S_{33} & 0 & 0 & 0 \\ 0 & 0 & 0 & S_{44} & 0 & 0 \\ 0 & 0 & 0 & 0 & S_{55} & 0 \\ 0 & 0 & 0 & 0 & 0 & S_{66} \end{bmatrix}^{(k)}. \tag{8}$$

To define the 3D laminated plate properties, the material modulus matrix elements S_{ij} (i, j=1,2,3) and S_{ii} (i=4,5,6) are needed. Their values can be calculated from elastic constants of the monolayer (E_L, E_T, E_r, G_{LT}, G_{Tr}, G_{rL}, μ_{LT}, μ_{Tr}, μ_{rL}), as shown in Eq.(9), and these elastic constants would be determined by Zheng *et al*.(2006).

$$\boldsymbol{S}^{(k)} = \begin{bmatrix} \frac{1}{E_L} & -\frac{\mu_{LT}}{E_T} & -\frac{\mu_{Lr}}{E_r} & 0 & 0 & 0 \\ -\frac{\mu_{TL}}{E_L} & \frac{1}{E_T} & -\frac{\mu_{Tr}}{E_r} & 0 & 0 & 0 \\ -\frac{\mu_{rL}}{E_L} & -\frac{\mu_{rT}}{E_T} & \frac{1}{E_r} & 0 & 0 & 0 \\ 0 & 0 & 0 & \frac{1}{G_{Tr}} & 0 & 0 \\ 0 & 0 & 0 & 0 & \frac{1}{G_{rL}} & 0 \\ 0 & 0 & 0 & 0 & 0 & \frac{1}{G_{LT}} \end{bmatrix}^{(k)}. \tag{9}$$

The on-axis stiffness matrix $\boldsymbol{C}^{(k)}$, is the inversion of on-axis flexibility matrix $\boldsymbol{S}^{(k)}$, written as

$$\boldsymbol{C}^{(k)} = (\boldsymbol{S}^{(k)})^{-1}. \tag{10}$$

The off-axis flexibility and stiffness matrices $\overline{\boldsymbol{S}}^{(k)}$ and $\overline{\boldsymbol{C}}^{(k)}$ can be calculated from the on-axis flexibility and stiffness matrices $\boldsymbol{S}^{(k)}$ and $\boldsymbol{C}^{(k)}$, by using flexibility and stiffness transformation matrices $\boldsymbol{T}_\varepsilon$ and $\boldsymbol{T}_\sigma$, respectively, written as,

$$\overline{\boldsymbol{S}}^{(k)} = \boldsymbol{T}_\varepsilon \boldsymbol{S}^{(k)} \boldsymbol{T}_\varepsilon^{\mathrm{T}}, \tag{11}$$

$$\overline{\boldsymbol{C}}^{(k)} = \boldsymbol{T}_\sigma \boldsymbol{C}^{(k)} \boldsymbol{T}_\sigma^{\mathrm{T}}, \tag{12}$$

where

$$\boldsymbol{T}_\varepsilon = \begin{bmatrix} m^2 & n^2 & 0 & 0 & 0 & -mn \\ n^2 & m^2 & 0 & 0 & 0 & mn \\ 0 & 0 & 1 & 0 & 0 & 0 \\ 0 & 0 & 0 & m & n & 0 \\ 0 & 0 & 0 & -n & m & 0 \\ 2mn & -2mn & 0 & 0 & 0 & m^2 - n^2 \end{bmatrix}, \tag{13}$$

$$\boldsymbol{T}_\sigma = \begin{bmatrix} m^2 & n^2 & 0 & 0 & 0 & -2mn \\ n^2 & m^2 & 0 & 0 & 0 & 2mn \\ 0 & 0 & 1 & 0 & 0 & 0 \\ 0 & 0 & 0 & m & n & 0 \\ 0 & 0 & 0 & -n & m & 0 \\ mn & -mn & 0 & 0 & 0 & m^2 - n^2 \end{bmatrix}, \tag{14}$$

where m=cosα, n=sinα, and α is the cylindrical angle of the steels from the pipe axis.

The relation of kth layer's stresses and strains between the cylindrical and material coordinates is respectively expressed as

$$\boldsymbol{\sigma}_z^{(k)} = \boldsymbol{T}_\sigma \boldsymbol{\sigma}_L^{(k)}, \tag{15}$$

$$\boldsymbol{\varepsilon}_z^{(k)} = \boldsymbol{T}_\varepsilon \boldsymbol{\varepsilon}_L^{(k)}. \tag{16}$$

The inner layer and outer layer represent isotropic, having the same stress-strain relations in any coordinate.

Global elastic constants

Based on the assumptions that all inter-laminar stresses are continuous across ply interfaces and that all in-plane strains are continuous through the thickness of composite laminates. Chou *et al.*(1972) presented a control volume approach to yielding a closed-form solution to determine global elastic constants for a laminated medium composed of individual layers.

The PSP's global stiffness matrix $\overline{\boldsymbol{C}}$ can be obtained by calculating the monolayers' off-axis stiffness matrices $\overline{\boldsymbol{C}}^{(2)}$ and $\overline{\boldsymbol{C}}^{(3)}$, the inner and outer

layers' stiffness matrices $\overline{\boldsymbol{C}}^{(1)}$ and $\overline{\boldsymbol{C}}^{(4)}$, the volume ratio of monolayers $V^{(2)}$ and $V^{(3)}$ and the volume ratio of inner and outer layers $V^{(1)}$ and $V^{(4)}$. The global stiffness constants $\overline{C}_{ij}$ can be expressed as follows (Chou *et al.*, 1972):

$$\overline{C}_{ij}=\sum_{k=1}^{4}V^{(k)}\left\{\overline{C}_{ij}^{(k)}-\frac{\overline{C}_{i3}^{(k)}\overline{C}_{3j}^{(k)}}{\overline{C}_{33}^{(k)}}+\frac{\overline{C}_{i3}^{(k)}\sum\limits_{l=1}^{4}\dfrac{V^{(l)}\overline{C}_{3j}^{(l)}}{\overline{C}_{33}^{(l)}}}{\overline{C}_{33}^{(k)}\sum\limits_{l=1}^{4}\dfrac{V^{(l)}}{\overline{C}_{33}^{(l)}}}\right\},$$
$$i,j=1,2,3,6, \tag{17}$$

where $V^{(2)}=V^{(3)}=t_c/(2t)$, $V^{(1)}=t_m/t$, $V^{(4)}=t_n/t$, and t_m, t_c, t_n is the thickness of the inner layer, winding layer, outer layer, respectively. t is the wall thickness of PSP.

$$\overline{C}_{ij}=\overline{C}_{ji}=0,\quad i=1,2,3,6;\ j=4,5, \tag{18}$$

$$\overline{C}_{ij}=\frac{\sum\limits_{k=1}^{4}\dfrac{V^{(k)}}{\Delta_k}\overline{C}_i^{(k)}}{\sum\limits_{k=1}^{4}\sum\limits_{l=1}^{4}\dfrac{V^{(k)}}{\Delta_k}\dfrac{V^{(l)}}{\Delta_l}(\overline{C}_{44}^{(k)}\overline{C}_{55}^{(l)}-\overline{C}_{45}^{(k)}\overline{C}_{54}^{(l)})},$$
$$i,j=4,5, \tag{19}$$

where

$$\Delta_k=\begin{vmatrix}\overline{C}_{44}^{(k)} & \overline{C}_{45}^{(k)}\\ \overline{C}_{54}^{(k)} & \overline{C}_{55}^{(k)}\end{vmatrix}=\overline{C}_{44}^{(k)}\overline{C}_{55}^{(k)}-\overline{C}_{45}^{(k)}\overline{C}_{54}^{(k)}. \tag{20}$$

The global flexibility matrix $\overline{\boldsymbol{S}}$ can be obtained by inversing the global stiffness matrix $\overline{\boldsymbol{C}}$. The global elastic constants are determined as

$$E_z=\frac{1}{\overline{S}_{11}},\ E_\theta=\frac{1}{\overline{S}_{22}},\ E_{rr}=\frac{1}{\overline{S}_{33}}, \tag{21}$$

$$\mu_{\theta z}=-\frac{\overline{S}_{21}}{\overline{S}_{11}},\ \mu_{r\theta}=-\frac{\overline{S}_{32}}{\overline{S}_{22}},\ \mu_{zr}=-\frac{\overline{S}_{13}}{\overline{S}_{33}}, \tag{22}$$

$$G_{z\theta}=\frac{1}{\overline{S}_{66}},\ G_{rz}=\frac{1}{\overline{S}_{55}},\ G_{\theta r}=\frac{1}{\overline{S}_{44}}. \tag{23}$$

Short-term burst pressure calculation

By analyzing the monolayer's mechanical properties with micro mechanics (Qiao, 1997), the monolayer's tensile strength in the L direction X_t, can be written as

$$X_t=X_{st}\upsilon_{st}+\sigma'_{PE,L}(1-\upsilon_{st}), \tag{24}$$

where $\sigma'_{PE,L}$ is the stress of PE in the L direction when steel wires break, MPa; υ_{st} is the ratio by volume of steel wires in PSP.

The thickness ratio is defined as the ratio between the outer and insider radii of PSP. For PSP with thickness ratio larger than 1.1, the thick wall analysis can satisfactorily be used. According to the Lame equation (Zheng *et al.*, 2001), the 3D stresses in the cylindrical coordinate can be described as

$$\sigma_\theta=\frac{PR_i^2}{R_o^2-R_i^2}+\frac{PR_o^2R_i^2}{R_o^2-R_i^2}\frac{1}{r^2}, \tag{25}$$

$$\sigma_r=\frac{PR_i^2}{R_o^2-R_i^2}-\frac{PR_o^2R_i^2}{R_o^2-R_i^2}\frac{1}{r^2}, \tag{26}$$

$$\sigma_z=\frac{PR_i^2}{R_o^2-R_i^2}, \tag{27}$$

where P is the internal pressure, MPa; R_o, R_i are the outer and insider radii of PSP, respectively, m; r is the radius of calculation position, m.

From the generalized Hooke's law, the 3D stains in the cylindrical coordinate are written as

$$\boldsymbol{\varepsilon}_z^{(k)}=\overline{\boldsymbol{S}}^{(k)}\boldsymbol{\sigma}_z^{(k)}. \tag{28}$$

Substituting Eqs.(25)~(27) into Eq.(28) and using Eqs.(21)~(23), the monolayer's strains $\boldsymbol{\varepsilon}_z^{(k)}$ are obtained. According to equation $\boldsymbol{\sigma}_z^{(k)}=\overline{\boldsymbol{C}}^{(k)}\boldsymbol{\varepsilon}_z^{(k)}$, which is from Eq.(1), the monolayer's stresses $\boldsymbol{\sigma}_z^{(k)}$, are obtained, then based on equation $\boldsymbol{\sigma}_L^{(k)}=\boldsymbol{T}_\sigma^{-1}\boldsymbol{\sigma}_z^{(k)}$, which is from Eq.(15), the monolayer's stresses $\boldsymbol{\sigma}_L^{(k)}$ are obtained.

The Maximum Stress Criterion considers that the material will fail as soon as one of the stresses exceeds the material's strength limit in its corresponding direction (Takayamagi *et al.*, 2002). For the monolayer studied in the paper, when $\sigma_L=X_t$, the steel wires break and then the PSP bursts. The short-term burst pressure of PSP can be described as

$$P_B = P_i R_c, \tag{29}$$

where P_B is the short-term burst pressure, MPa; P_i is the initial value of the short-term burst pressure, MPa; R_c is the strength ratio ($R_c = X_t/\sigma_L$).

Based on the analysis above, the short-term burst pressure of PSP can be calculated according to Fig.4.

EXPERIMENTAL INVESTIGATION

Material test

The materials of PSP are the steel wire and high density polythene (HDPE). After the material test according to the Chinese Standards GB/T228-2002 (2002) and GB/T8804.3-2003 (2003), mechanical properties of the steel wire and HDPE were obtained, as shown in Table 1.

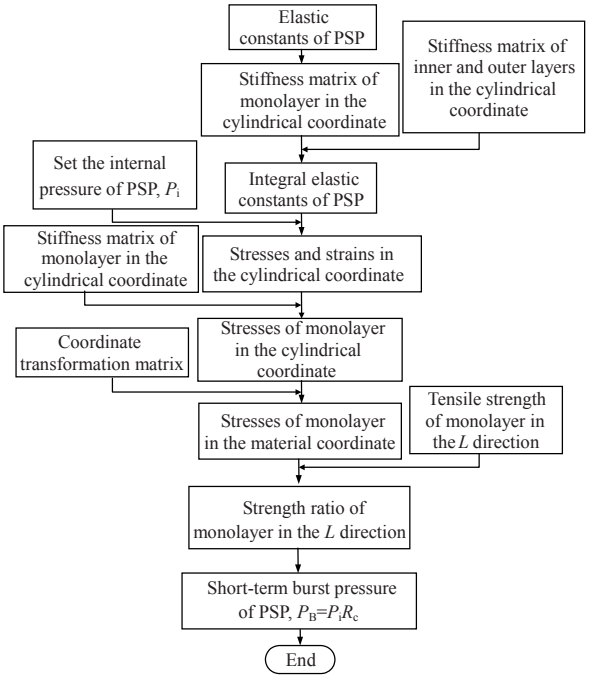

Fig.4 Flow chart for calculating short-term burst pressure

Table 1 Material properties

Material	Tensile rength (MPa)	Percentage of breaking elongation (%)	Poisson's ratio
Steel wire	1832	5	0.26
HDPE*	26.5	785	0.45

* HDPE: high density polythene

Burst test

To prove availability of the presented analysis, burst test was carried out on 20 types of PSP at room temperature (25 °C), and each type includes four specimens. The parameters of outer radius (*DN*), wall thickness (*t*), steel wire's diameter (*d*), winding steel wires' amount (*N*) are listed in Table 2, and these specimens have the uniform winding angle of 54.7°.

In order to study the effect of reinforcement of the steel wire mesh skeleton, the burst test was performed on four PE specimens having an outer radius (*DN*) of 250 mm, a wall thickness (*t*) of 15 mm. The comparable specimen of PSP is Type 15 (Table 2).

The specimens were pressurized with a hydraulic pump. The flows of fluid were regulated through a non-return valve. Experimental equipment is sealed by clamping fixtures, which are a type of the Chinese Standards GB6111-2003 (2003), as shown in Figs.5 and 6. The test method refers to Chinese Standards GB/T15560-95 (1995). The specimens were continuously pressurized till they burst and the short-term burst pressure values were recorded. The

Table 2 Parameters of specimens

Type No.	*DN* (mm)	*d* (mm)	*N*	*t* (mm)	Type No.	*DN* (mm)	*d* (mm)	*N*	*t* (mm)
1	110	0.8	36	8.5	11	200	1.0	120	10.5
2	110	0.8	56	10.0	12	200	1.0	160	10.5
3	160	0.8	60	9.5	13	250	0.8	100	12.0
4	160	0.8	90	10.0	14	250	0.8	200	12.5
5	160	1.0	60	9.5	15	250	1.0	200	16.0
6	160	1.0	144	10.0	16	250	1.2	200	15.0
7	200	0.8	80	11.0	17	315	0.8	210	12.5
8	200	0.8	120	10.5	18	315	0.8	280	12.5
9	200	0.8	160	10.5	19	400	1.0	320	15.0
10	200	1.0	100	10.0	20	500	1.0	384	16.0

DN: outer radius of PSP; *d*: steel wire's diameter; *N*: winding steel wires' amount; *t*: wall thickness of PSP

experimental data of short-term burst pressure of each type shown in Table 3 is the average value of four specimens' experimental data.

RESULTS

The short-term burst pressure is calculated using the mechanical properties of material (Table 1) and the parameters of PSP (Table 2). The theoretical data and experimental data are both listed in Table 3, and the comparison between theoretical and experimental data indicates that there is a good agreement between them. The absolute error range is −0.3 MPa~0.2 MPa, the relative error range is −5%~4.1%, the average value of relative error is −0.65%, and the quadratic sum of relative error is 0.0154.

Average short-term burst pressure of PE pipe at room temperature is 3.4 MPa and that of PSP is 7.8 MPa. That is to say, the latter is 129% higher than the former. Accordingly, the steel wire mesh skeleton can enhance the burst resistance of the pipes effectively.

Fig.5 Equipment for burst test

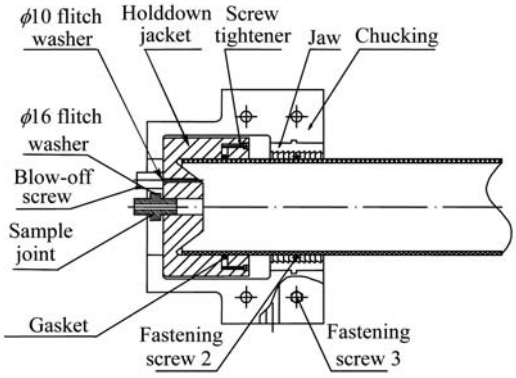

Fig.6 Inlet end of the equipment for burst test

DISCUSSION

With the increasing of internal pressure on the test, the PSP deformed uniformly. A crack of steel wire break was heard when the internal pressure was close to the short-term burst pressure and the PSP burst subsequently. After observing the crevasse, we found that the steel wire was breaking, which demonstrated that the stresses of steel wires had reached their tensile strength. The plastic of this region was mainly lacerated and had a few rough edges, belonging to ductile burst.

The burst shape of PSP takes on some forms due to practical manufacture technics, especially the uniformity of steel wire's spacing. This paper gives some burst shapes (Fig.7). The straight burst is 375 mm in length (Fig.7a); The U shaped burst is 455 mm in length (Fig.7b).

We found that the distribution of steel wires is not uniform in some regions due to the imperfect winding (Fig.8). The uniformity of steel wire's

Table 3 Theoretical and experimental data of short-term burst pressure

Type No.	Theoretical data (MPa)	Experimental data (MPa)	Absolute error (MPa)	Relative error (%)	Type No.	Theoretical data (MPa)	Experimental data (MPa)	Absolute error (MPa)	Relative error (%)
1	6.0	6.3	−0.3	−4.8	11	5.8	5.9	−0.1	−1.7
2	8.0	8.0	0.0	0.0	12	7.0	7.0	0.0	0.0
3	4.5	4.4	0.1	2.3	13	3.3	3.4	−0.1	−2.9
4	5.5	5.7	−0.2	−3.5	14	4.5	4.6	−0.1	−2.2
5	5.5	5.6	−0.1	−1.8	15	6.6	6.6	0.0	0.0
6	9.5	9.4	0.1	1.1	16	8.1	8.0	0.1	1.3
7	4.0	4.2	−0.2	−4.8	17	3.2	3.2	0.0	0.0
8	4.5	4.4	0.1	2.3	18	3.7	3.8	−0.1	−2.6
9	5.3	5.2	0.1	1.9	19	3.8	4.0	−0.2	−5.0
10	5.1	4.9	0.2	4.1	20	3.0	2.9	0.1	3.4

spacing is a very important factor which affects the burst shape of PSP significantly.

1. Straight burst (Fig.9a)

Assume that the steel wire's spacing is uniform and the 4th steel wire breaks at the point of *a* firstly, then the stress of the 7th steel wire will reach the limit strength and breaks subsequently. Through the similar analysis, we can obtain that the next breaks of steel wires will happen at the *b* and *c* points, respectively. Therefore, the straight burst will appear when the steel wire's spacing is uniform.

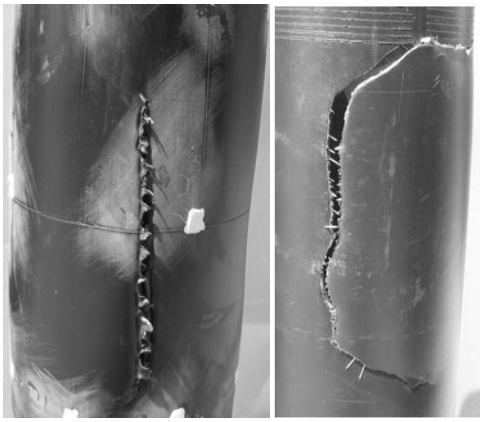

(a) (b)

Fig.7 Two burst modes of PSP at room temperature (25 °C). (a) Straight burst; (b) U shaped burst

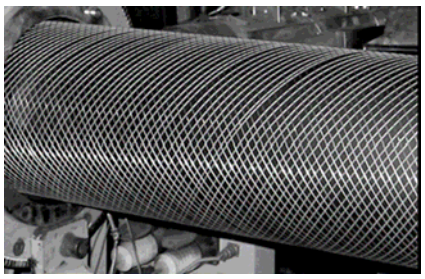

Fig.8 Distribution of steel wires in manufacture

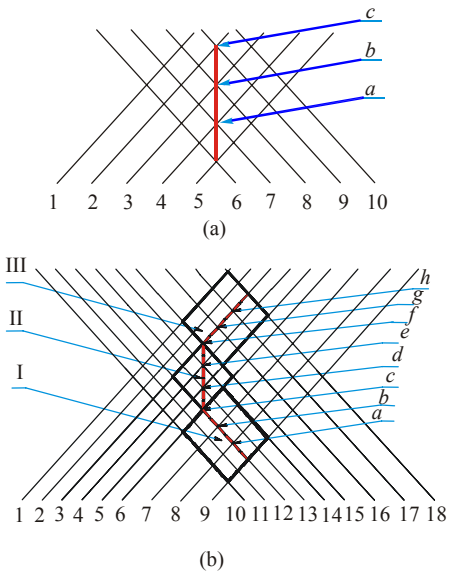

Fig.9 Schematic illustration of the distribution of steel wires. (a) Straight burst; (b) U shaped burst

2. U shaped burst (Fig.9b)

Assume that the steel wire's spacing is not uniform in regions of I and III. In Region I, because of the symmetric winding, the total load of four steel wires (6th~9th) is almost equal to that of five steel wires (10th~14th), so the stress of the 6th~9th steel wires is larger than that of the 10th~14th steel wires, which lead to the fact that the 6th~9th steel wires break at *a*, *b* and *c* points, respectively. In Region III, through the similar analysis, we can obtain that the 15th~18th steel wires break at *f*, *g* and *h* points, respectively. In Region II, the steel wire's spacing is uniform, so there will appear the straight burst (the straight line of *c-d-e-f*) in this region.

CONCLUSION

This paper presents a solution to predict the short-term burst pressure of PSP based on the assumption of an orthotropic material model for the monolayer. Through a 3D analysis and an experimental investigation, the following conclusions were obtained:

(1) By applying the anisotropic elasticity and Maximum Stress Failure Criterion, a theoretical approach to calculating the short-term burst pressure of PSP is obtained. Good agreement between theoretical results and experimental data shows that the proposed approach can well predict short-term burst pressure of PSP.

(2) Burst test was carried out on PE pipes at room temperature and experimental results show that short-term burst pressure of PSP at room temperature is increased by 129% comparing with that of PE pipes. Therefore, the effect of reinforcement of the steel wire mesh skeleton is obvious.

References

Chinese Standards GB/T15560-1995, 1995. Standard Test Method for Short-time Hydraulic Failure and Resistance to Constant Internal Pressure of the Plastics Pipes for the

Transport of Fluids (in Chinese).

Chinese Standards GB/T228-2002, 2002. Metallic Materials-tensile Testing at Ambient Temperature (in Chinese).

Chinese Standards GB/T8804.3-2003, 2003. Test Methods of Tensile Properties for Thermoplastic Pipes—Polyolefin Pipes (in Chinese).

Chinese Standards GB6111-2003, 2003. Thermoplastics Pipes for the Conveyance of Fluids-resistance to Internal Pressure-test Method (in Chinese).

Chou, P.C., Carleone, J., Hsu, C.M., 1972. Elastic constants of layered media. *Journal of Composite Materials*, **6**(1):80-93. [doi:10.1177/002199837200600107]

Hwang, T.K., Hong, C.S., Kim, C.G., 2003. Probabilistic deformation and strength prediction for a filament wound pressure vessel. *Composites Part B*: *Engineering*, **34**:481-497.

Kobayashi, S., Imai, T., Wakayama, S., 2007. Burst strength evaluation of the FW-CFRP hybrid composite pipes considering plastic deformation of the liner. *Composites Part A*: *Applied Science and Manufacturing*, **38**(5):1344-1353. [doi:10.1016/j.compositesa.2006.10.011]

Kruijer, M.P., Warnet, L.L., Akkerman, R., 2006. Modelling of the viscoelastic behaviour of steel reinforced thermoplastic pipes. *Composites Part A*: *Applied Science and Manufacturing*, **37**(2):356-367. [doi:10.1016/j.compositesa.2005.04.019]

Lu, Y.B., Ma, X., Fang, X.B., Chen, Z.W., Zheng, J.Y., Qiu, S.L., 2005. The research advances in plastic-matrix metal composite pipe. *Chemical Engineering and Machinery*, **32**(2):125-128 (in Chinese).

Parnas, L., Katirci, N., 2002. Design of fiber-reinforced composite pressure vessels under various loading conditions. *Composite Structures*, **58**(1):83-95. [doi:10.1016/S0263-8223(02)00037-5]

Qiao, S.R., 1997. Micro Mechanics Property of Composite Meterial. Northwesten Polytechnical University Press, Xi'an, p.20-37 (in Chinese).

Takayanagi, H., Xia, M., Kemmochi, K., 2002. Stiffness and strength of filament-wound fiber-reinforced composite pipes under internal pressure. *Advanced Composite Materials*, **11**(2):137-149. [doi:10.1163/156855102760410333]

Uemura, M., Fukunaga, H., 1981. Probabilistic burst strength of filament wound cylinders under internal pressure. *Journal of Composite Materials*, **15**(5):462-480. [doi:10.1177/002199838101500505]

Xia, M., Kemmochi, K., Takayanagi, H., 2001. Analysis of filament-wound fiber-reinforced sandwish pipe under combined internal pressure and thermomechanical loading. *Composite Structures*, **51**(3):273-283. [doi:10.1016/S0263-8223(00)00137-9]

Xia, M., Takayanagi, H., Kemmochi, K., 2001. Analysis of multi-layered filament-wound composite pipes under internal pressure. *Composite Structures*, **53**(4):483-491. [doi:10.1016/S0263-8223(01)00061-7]

Zheng, J.Y., Dong, Q.W., Sang, Z.F., 2001. Process Equipment and Design. Chemical Industry Press, Beijing, p.43-48 (in Chinese).

Zheng, J.Y., Lin, X.F., Lu, Y.B., Li, X., Zhu, Y.C., Xu, P., Sun, G.Y., 2006. Stress Analysis of Plastic Pipe Reinforced by Cross Helically Wound Steel Wires. ASME Pressure Vessel and Piping Division Conference.

Zheng, J.Y., Lu, Y.B., Li, X., Lin, X.F., Zhu, Y.C., Xu, P., Chen, D.F., He, X.L., Shao, T.Q., 2007. Experimental investigation on mechanical properties of plastic pipes reinforced by cross helically wound steel wires. *Pressure Vessel and Technology* (in Press)